8th European Workshop On Structural Health Monitoring (EWSHM 2016), 5-8 July 2016, Spain, Bilbao
www.ndt.net/app.EWSHM2016

Recognition of Rebar and Crack Based on Impact-Echo Phase Analysis

Pei-Ling, Liu [1], Li-Chuan, Lin [2], Ying-Yan, Hsu [3], Cheng-Yu, Yeh [4], Po-Liang, Yeh *[5]

[1] Institute of Applied Mechanics, National Taiwan University. No.1, Sec. 4, Roosevelt Rd., Da'an Dist. Taipei City 106, Taiwan. peiling@ntu.edu.tw
[2,3,4] Institute of Applied Mechanics, National Taiwan University. No.1, Sec. 4, Roosevelt Rd., Da'an Dist. Taipei City 106, Taiwan.
[5] Institute of Applied Mechanics, National Taiwan University. No.1, Sec. 4, Roosevelt Rd., Da'an Dist. Taipei City 106, Taiwan. d88543003@ntu.edu.tw

Abstract

The impact-echo test is often adopted to detect the defects or inclusions in concrete structures. Applying Fourier transform to the surface response of the target structure due to an impact, the depth of the interface can be determined by applying the impact-echo equation. Although the impact echo spectrum may disclose the existence of an interface in the structure, it cannot tell whether the interface comes from a crack or a rebar. Such information is crucial in the safety assessment of the structure. It is also necessary in the determination of interface depth, because the impact-echo equations for crack and rebar differ.

The objective of this study is to develop an index that can be used to differentiate crack echo from rebar echo. The idea is based on the phase change of the reflected wave. As a wave encounters a hard interface, it reflects with a phase change of π, but as it encounters a soft interface, there is no phase change. Hence, it is proposed that both the magnitude and phase spectra are constructed in the Fourier analysis of the impact-echo signals. Determine the frequency of the interface echo using the magnitude spectrum. Then, use the phase at the echo frequency in the phase spectrum to determine whether the echo is from a crack or a rebar. Numerical and experimental tests were performed to verify the proposed method. As expected, the phases of crack echoes are closer to 0, while the phases of rebar echoes are closer to π/2. The phase at the echo frequency in the phase spectrum appears to be an effective index in determining the type and depth of the interface in the concrete.

Key words: Impact-echo test, Nondestructive test, Phase, Crack, Rebar.

1. INTRODUCTION

The impact echo test is widely applied in the nondestructive testing of concrete structures. It was primarily applied to detect internal flaws in concrete plate [1, 2]. Later, it was used to inspect the flaws in rod structures, concrete panels, and the corrosion damage of rebar in concrete [3-6].

In the impact echo test, a steel ball is used to produce an impact source on the surface of the concrete specimen, and a transducer is placed near the impact source to receive the surface response of the structure. The received time signals are recorded for data analysis. Then, Fourier transform is utilized to transform the time signal to frequency domain.

When a wave propagates in a structure, it reflects as it encounters an interface. Then the reflected wave rebounds back to the surface and reflect again into the interior of the structure. The process repeats and multiple reflections occur between the surface and the interface until the wave fades out. Hence, an echo peak is formed in the Fourier spectrum. The peak frequency *f* is related to the depth of the interface *D* by the following equations [1]:

$$D = \frac{C_p}{kf} \qquad k = \begin{cases} 2 & \text{for crack interface} \\ 4 & \text{for rebar interface} \end{cases} \tag{1}$$

where C_p is the velocity of the longitudinal wave. Thus, by locating the peaks in the Fourier spectrum, the depth of an internal crack or a rebar can be determined.

Although the Fourier spectrum of the impact-echo signal may disclose the existence of an interface in the structure, one cannot tell whether the interface is caused by a crack or a rebar. Such information is crucial in the safety assessment of the structure. It is also required in the selection of *k* value in Eq. (1). Only a few researchers have addressed this issue in the past 3 decades. Kuo et al. [7] applied the empirical mode decomposition (EMD) to find the response difference between cracks and rebars. Liu & Yeh [8] showed that crack and rebar echoes exhibit different patterns in the bispectrum. Ke [9] conducted numerous numerical tests and model tests to verify the feasibility of bispectrum in recognizing crack and rebar echoes. Although some classification features were noted in these studies, no clear index was proposed to classify the interface.

This research aims at developing a method that is able to differentiate crack echo from rebar echo easily. In contrast to the aforementioned researches, a simple index will be proposed. As such, the classification will not rely on the investigator's subjective judgement. The idea is based on the phase change of the reflected wave. The details are as follows.

2. IMPACT-ECHO PHASE ANALYSIS

2.1 Magnitude and phase spectra

The Fourier transform of a time signal $x(t)$ is as follows:

$$X(f) = \int_{-\infty}^{+\infty} x(t) e^{-2i\pi ft} dt \tag{2}$$

$X(f)$ is a complex function, and it can be written as

$$X(f) = \int_{-\infty}^{+\infty} x(t)[\cos(2\pi ft) - i\sin(2\pi ft)]dt = X_{\mathrm{Re}}(f) + iX_{\mathrm{Im}}(f) \tag{3}$$

$X(f)$ can alternately be expressed in the polar form as

$$X(f) = \sqrt{X_{\mathrm{Re}}^2(f) + X_{\mathrm{Im}}^2(f)} e^{i\varphi(f)} = |X(f)| e^{i\varphi(f)} \tag{4}$$

$$\varphi(f) = \tan^{-1}\left\{\frac{X_{\mathrm{Im}}(f)}{X_{\mathrm{Re}}(f)}\right\} \tag{5}$$

where $X_{\mathrm{Re}}(f)$ and $X_{Im}(f)$ are the real and imaginary parts of $X(f)$; $|X(f)|$ and $\varphi(f)$ respectively are the magnitude spectrum and phase spectrum of the signal.

If $\varphi(f)$ is replaced by $\varphi(f) + 2\pi k$ in Eq. (4), where k is any integer, $X(f)$ remains unchanged. Hence, the phase function $\varphi(f)$ is often restricted to the range $[-\pi, \pi]$, called the wrapped phase. If the actual phase is outside this range, it is increased or decreased by a multiple of 2π to keep the phase value within the $[-\pi, \pi]$ range.

2.2 Phase of simplified echo data

Consider a uniform medium bounded by two parallel planes. The thickness of the medium is *D*. The top and bottom surfaces of the medium is traction free. The bottom resembles a concrete-crack interface. Let a compressive plane wave enter the medium at right angle. The longitudinal wave (P wave) changes sign when it encounters the bottom free surface. Hence, the incident compressive stress is reflected as a tensile stress wave. As the tensile stress wave reaches the top surface, it reflects as a compressive stress wave. The cycle of compressive and tensile stress waves repeats and multiple reflections occur between the top and the bottom. The resulted vertical displacement at the top surface is schematically shown in Fig. 1(a). It is a periodic function with frequency $f_0 = C_p / 2D$, according to Eq. (1).

On the other hand, consider a second medium of thickness *D*/2. Its bottom is not traction-free but bonded to a material with higher acoustic impedance, resembling a concrete-rebar interface. The incident compressive stress wave remain a compressive stress wave as it reflects from the bottom interface. When the compressive stress wave reaches the top free surface, it reflects as a tensile stress wave. The vertical displacement at the top surface is schematically shown in Fig. 1(b). Although the thickness of the second medium is only one half the thickness of the first medium, the frequency of the periodic displacement curve is still $C_p / 2D$, according to Eq. (1).

Now, simplify the vertical displacement at the top surface of the first medium as a sequence of half-sines, i.e.,

$$x_c(t) = -\left|\sin(\pi f_0 t)\right| \tag{6}$$

and the vertical displacement at the top surface of the second medium as a sine wave, i.e.,

$$x_s(t) = -\sin(2\pi f_0 t) \tag{7}$$

.

The Fourier transform of $x_c(t)$ and $x_s(t)$ are as follows:

$$X_c(f) = -\frac{2}{\pi}\delta(f) + \sum_{n=1}^{\infty}\frac{4}{(4n^2-1)}\left[\delta(f - nf_0) + \delta(f + nf_0)\right] \tag{8}$$

$$X_s(f) = i\pi\left[\delta(f - f_0) - \delta(f + f_0)\right] \tag{9}$$

Since $X_c(f)$ is real and $X_s(f)$ is imaginary, according to Eq. (5), the phases of $X_c(f)$ and $X_s(f)$ at $f = f_0$ are respectively

$$\varphi_c(f_0) = 0 \tag{10}$$

$$\varphi_s(f_0) = \frac{\pi}{2} \tag{11}$$

Notice that there is no attenuation in $x_c(t)$ and $x_s(t)$. That is not true for real signals. To take attenuation into account, $x_c(t)$ and $x_s(t)$ are modified as follows:

$$x_c(t) = -e^{-2\pi\varsigma f_0 t}\left|\sin(\pi f_0 t)\right| = -r^{f_0 t}\left|\sin(\pi f_0 t)\right| \tag{12}$$

$$x_s(t) = -e^{-2\pi\varsigma f_0 t}\sin(2\pi f_0 t) = -r^{f_0 t}\sin(2\pi f_0 t) \tag{13}$$

where ζ is the damping ratio, and $r = e^{-2\pi\varsigma}$ is the ratio of two consecutive wave amplitudes. The waveforms of $x_c(t)$ and $x_s(t)$ and the definition of *r* are as shown in Fig. 2.

One can show that

$$\varphi_c(f_0) = \tan^{-1}\left\{\frac{8\varsigma}{3-4\varsigma^2}\right\} \tag{14}$$

$$\varphi_s(f_0) = \tan^{-1}\left\{\frac{2}{\varsigma}\right\} \tag{15}$$

For $r = 1.0 \sim 0.5$, $\varphi_c(f_0) = 0 \sim 0.09\pi$ and $\varphi_s(f_0) = 0.5\pi \sim 0.52\pi$, still very close to 0 and $\pi/2$, respectively. It can be concluded that the phase at the echo frequency is approximately 0 or $\pi/2$, depending on the type of interface at the bottom of the medium.

It seems that $\varphi(f_0)$ is a good indicator of the type of interface. However, this conclusion are derived based on the simplified signals. In the following, the simulated impact echo data will be analyzed to see if $\varphi(f_0)$ still works in the identification of the interface type.

3. NUMERICAL TESTS

The finite element code LS-Dyna971 [10] was adopted to simulate the response of concrete specimens due to the impact of a steel ball.

The dimensions of the concrete specimens are identically 80 cm (L) × 80 cm (W) × 20 cm (H). The specimens either contain a 32 cm (L) × 32 cm (W) × 1 cm (H) horizontal crack or a 3 cm diameter steel rebar. Three dimensional solid elements with side length 1 cm were used in the simulation. The Young's modulus, mass density, Poisson's ratio, and longitudinal wave speed were 33.1 GPa, 2300 kg/m3, 0.2, and 4000 m/s, respectively, for the concrete, and 207 GPa, 7850 kg/m3, 0.28, and 5800 m/s, respectively, for the rebar. Absorbing boundary conditions were applied on the four sides of the models to simplify the wave behavior.

Six inclusion cases were considered, namely, 1. an 8 cm deep crack, 2. a 10 cm deep crack, 3. a 12 cm deep crack, 4. a 4 cm deep rebar, 5. a 5 cm deep rebar, and 6. a 6 cm deep rebar. Notice that cases 1 and 4 have the same echo frequency, so do cases 2 and 5, and cases 3 and 6. For each inclusion case, tests were conducted at two different locations on the top surface, right above the inclusion.

A time-varying pressure was applied to the surface on an element facet to simulate the impact of a steel ball with diameter *d* = 6 mm. The pressure was approximated by a half sine function with a contact time $t_c = 25\mu s$. The vertical displacement of a node 3.5 cm away from the impact source was recorded. The total simulation time was 3 msec, and the time interval was 3 msec/1024 = 2.93 μsec.

Figures 3 and 4 show the response of the specimens obtained in the numerical tests of cases 3 and 6. In both cases, the direct longitudinal wave is followed by a very strong surface wave in both cases. During that period of surface wave, the echo from the crack is not observable. The surface wave is often removed from the signal in impact echo analysis because it may complicate the Fourier spectrum.

Since this study tries to use the phase spectrum to differentiate crack and rebar interfaces, the removal of a segment of signal must be conducted carefully. To keep the phase at the echo frequency unchanged, we only remove a multiple of the echo period from the signal, i.e., n/f_0, where *n* is an integer. Since the echo signal decays quickly, the signal removed should be as short as possible, just long enough to span the surface wave.

Figure 5 shows the distribution of $\varphi(f_0)$ of the numerical tests. The phase offsets of crack echoes range from -0.05π to 0.17π; while the phase offsets of rebar echoes range from 0.34π to 0.54π. Although not all phases are nearly 0 or 0.5π, the data points are clearly divided into two groups. For the crack cases, $\varphi_c(f_0)$'s are closer to 0; for the rebar cases, $\varphi_s(f_0)$'s are closer to $\pi/2$. One can easily find a dividing line to seperate the crack and rebar data points.

4. MODEL TESTS

In this study, model tests were also conducted on 4 concrete specimens to verify the feasibility of the proposed method. The dimensions of the specimens are identically 80 cm (L) × 80 cm (W) × 20 cm (H). The inclusions in the specimens are: 1. a 12 cm deep horizontal crack, 2. an inclined crack with depth 8 ~ 12 cm, 3. a 6 cm deep rebar, and 4. a 3 cm deep rebar. For each inclusion case, tests were conducted at three different locations on the top surface, right above the inclusion.

A steel ball was dropped on the surface to produce an impact on the specimen. A conical transducer located 4 cm away from the impact point was adopted to measure the vertical displacement on the concrete surface. The received voltage signals were recorded by a digital oscilloscope. The sampling rate was 2 MHz, and the total sampling time was 5 msec. Since the impact source varies in the experiments, tests were repeated 5 times at each test location.

Figure 6 shows the $\varphi(f_0)$ of the model tests. Similar to the numerical tests, the data points are clearly divided into two groups. In fact, the two groups of data points are even farther apart in Fig. 6 than in Fig. 5. Hence, the type of the interface can be determined without difficulty. $\varphi(f_0)$ appears to be a good index for the classification of inclusions, and $\varphi(f_0) = \pi/4$ seems to be a good decision line.

5. CONCLUSION

This study develops a method to differentiate the echoes from crack and rebar interfaces in concrete structures based on the phase spectrum of the impact echo signals. Analysis of the simplified reflection signals suggests that the phase at echo frequency is nearly 0 for crack interface and nearly $\pi/2$ for rebar interface. Both numerical and experimental tests were conducted to verify the discovery. As expected, the data points can be successfully divided into two groups: the phase offsets of crack echoes are closer to 0, while the phase offsets of rebar echoes are closer to $\pi/2$. Furthermore, $\varphi(f_0) = \pi/4$ seems to be a good decision line for the type of interface.

Hence, it is proposed that both the magnitude and phase spectra be constructed in the Fourier analysis of the impact-echo signals. One may use the magnitude spectrum to determine the echo frequency and use the phase spectrum to determine type of inclusion. Then, choose the right equation to compute the depth of inclusion. As such, one can get both the type and depth of the inclusion correctly.

ACKNOWLEDGE

The authors thank the National Science Council of Taiwan, for the financial support through the Grants NSC 98-2221-E-002-104-MY3.

REFERENCES

[1] Sansalone, M. and N.J. Carino, Impact-Echo:A Method for Flaw Detection in Concrete Using Transient Stress Waves. NBSIR 86-3452. 1986, Gaithersburg, MD:National Bureau of Standard 222.

[2] Lin, Y., Sansalone M. & Carino N. J., Finite Element Studies of the Transient Response of Plates Containing Thin Layers and Voids. J. Nondestructive Evaluation, 1990. 9(1): p. 27-47.

[3] Lin, Y. and M. Sansalone, Transient Response of Thick Circular and Square Bars Subjected to Transverse Elastic Impact. J. Acoustical Society of America, 1992. 91(2): p. 885-893.

[4] Cheng, C. and M. Sansalone, The Impact-Echo Response of Concrete Plates Containing Delaminations: Numerical, Experimental and Field Studies. Material and Structures, 1993. 26: p. 274-285.

[5] Cheng, C. and M. Sansalone, Effects on Impact-Echo Signals Caused by Steel Reinforcing Bars and Voids around Bars. ACI Materials Journal, 1993. 90(5): p. 421-434.

[6] Liang, M.-T. and P.-J. Su, Detection of the Corrosion Damage of Rebar in Concrete Using Impact-Echo Method. Cement and Concrete Research, 2001. 31(10): p. 1427~1436.

[7] Kuo, J.C., P.L. Liu, and P.L. Yeh, Distinction of Rebar and Crack Echoes in Impact Echo Signals Using Empirical Mode Decomposition, in Nondestructive detection conference 2008. Taiwan, Nantou.

[8] Liu, P.L. and P.L. Yeh, Application of bispectrum in recognizing rebar and crack based on impact-echo test, in The 15th Conference on Nondestructive Testing. 2010: Kaohsiung city, Taiwan.

[9] Ke, C.H., Application of bispectrum in the impact-echo method to identify reinforcing steel bar and crack, in Institute of applied mechanics. 2012, National Taiwan University

[10] Hallquist, J.O., LS-DYNA Keyword User's Manual. 2003, Livermore: Livermore Software Technology Corporation.

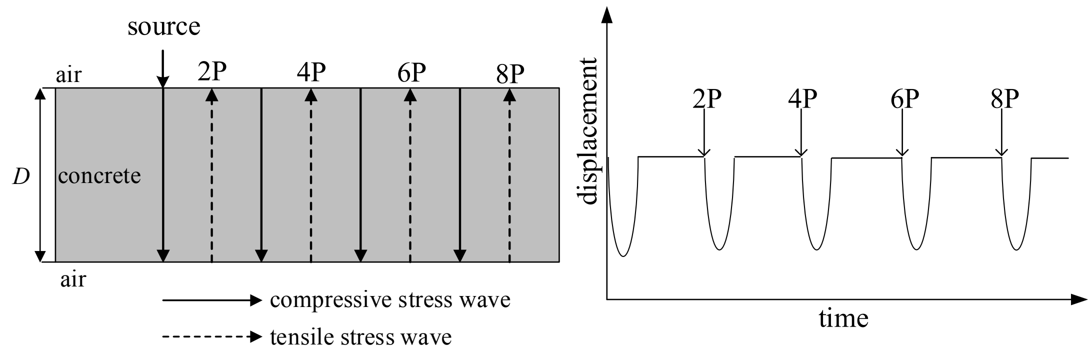

(a) concrete-crack interface

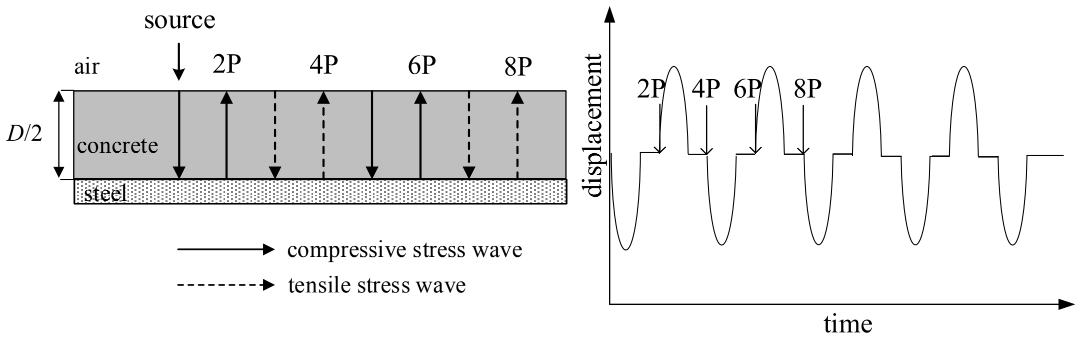

(b) concrete-rebar interface

Fig. 1 Influence of interface type on the echo signals

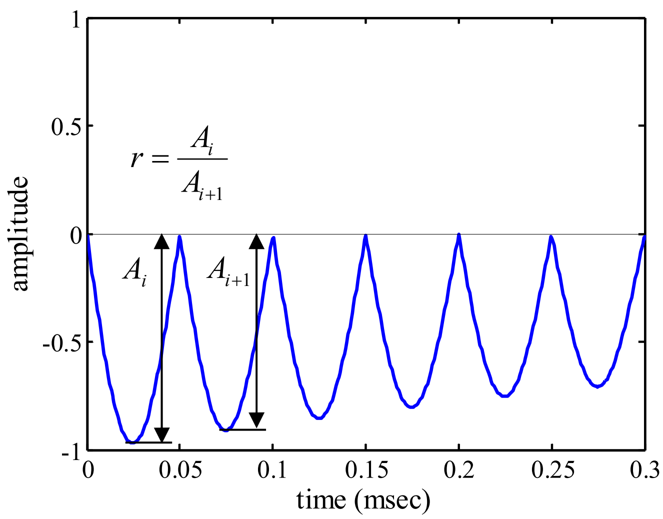

(a) concrete-crack interface

Fig. 2 Simplified echo signals

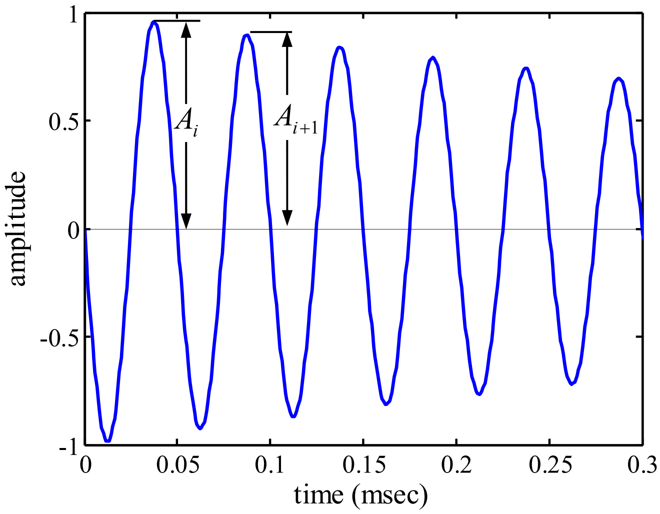

(b) concrete-rebar interface

Fig. 2 Simplified echo signals (cont'd)

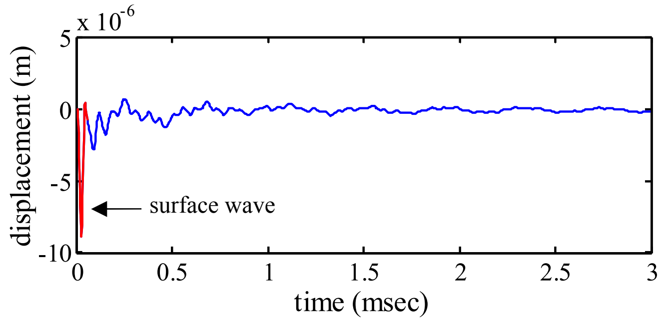

(a) vertical displacement

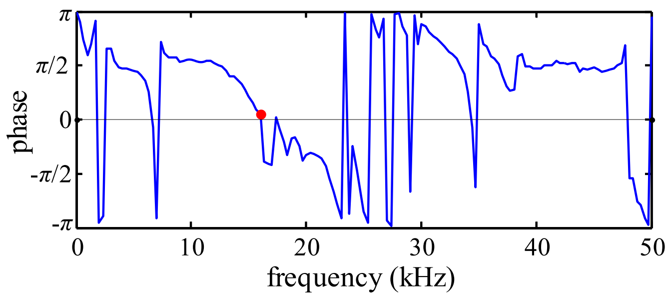

(b) phase spectrum

Fig. 3 Response of the specimen with a 12 cm deep crack

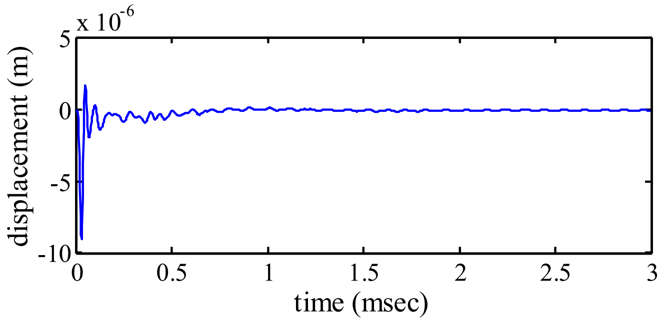

(a) vertical displacement

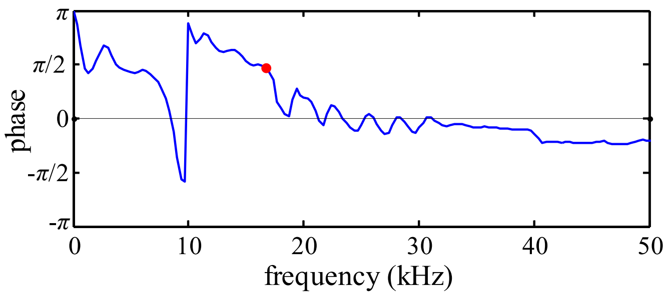

(b) phase spectrum

Fig. 4 Response of the specimen with a 6 cm deep rebar

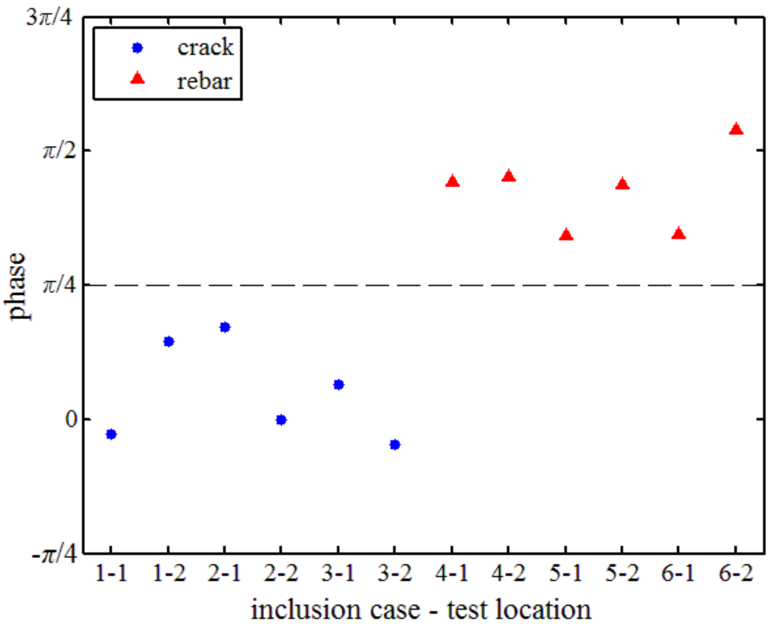

Fig. 5 Results of numerical tests

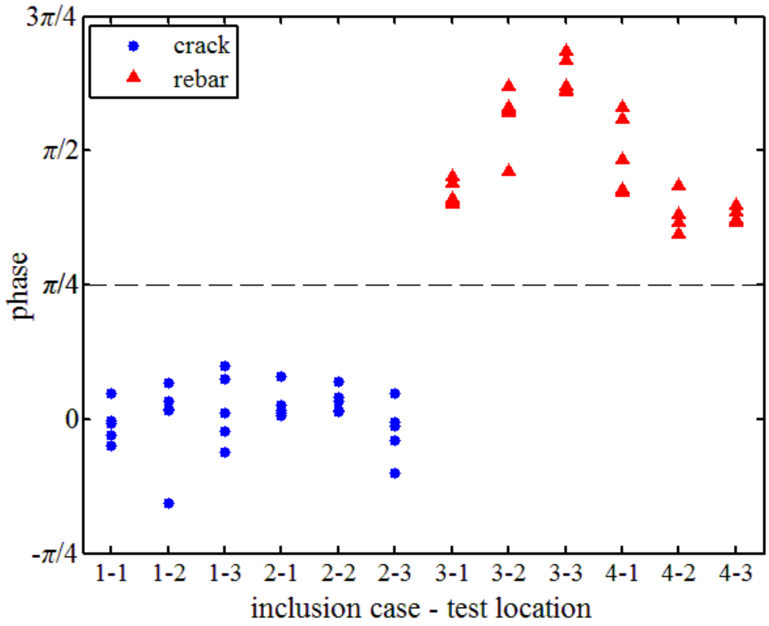

Fig. 6　Results of model tests